

IAC-14-B4.7B.6

CALIBRATION APPROACH OF THE OLFAR SPACE-BASED RADIO TELESCOPE

P. K. A. van Vugt

University of Twente, Telecommunication Engineering Group, The Netherlands, p.k.a.vanvugt@utwente.nl

A. Budianu

University of Twente, Telecommunication Engineering Group, The Netherlands, a.budianu@utwente.nl

A. Meijerink

University of Twente, Telecommunication Engineering Group, The Netherlands, a.meijerink@utwente.nl

M. J. Bentum

University of Twente, Telecommunication Engineering Group, The Netherlands, m.j.bentum@utwente.nl
ASTRON, The Netherlands

In recent years, science drivers have emerged for radio astronomy in the frequency range between 0.3 and 30 MHz. Due to strong man-made radio frequency interference (RFI) and opacity and scintillation in the ionosphere, this is not possible on Earth. For this reason the Orbiting Low-Frequency Antennas for Radio Astronomy (OLFAR) project aims to develop a space-based radio telescope, consisting of 50 or more nano-satellites in a location far away from Earth. These satellites will be flying in a swarm approximately 100 km in diameter to synthesize a large radio aperture. As with any radio telescope, OLFAR will need to be calibrated. However the satellite swarm concept brings along several unique challenges for the calibration, which are outlined in this paper. An approach is proposed for the calibration using known calibrator sources and an alternating least squares (ALS) approach which solves for the complex receiver gains, the array response matrix, direction dependent antenna gains towards the calibrator sources and the receiver noise power. This paper provides proof of concept of the proposed calibration approach by means of Monte Carlo simulations.

I. INTRODUCTION

The frequency range between 0.3 and 30 MHz is one of the last radio frequency bands that have not yet been properly explored by radio telescopes. However, it is expected that a lot of new scientific information can be discovered at those frequencies. The main science driver is cosmology. Specifically finding out what happened in the early universe, during the 'Dark Ages', which is between the moment of cosmic background radiation (0.38 million years after the Big Bang) and Epoch of Reionization (400 million years after the Big Bang). Other applications of such a radio telescope include Extragalactic and Galactic Surveys and to record Transients, such as pulsar signals, solar or planetary bursts, and low-frequency signals from (exo-)planets^{1,2}.

The reason why this frequency range has never been explored before is that the ionosphere causes scintillation roughly between 10 and 30 MHz, and is becoming completely opaque below 10 MHz. Man-made interference is also prohibitively severe at these frequencies, not only on the Earth's surface, but even in high Earth orbit². Hence OLFAR needs to be placed in a location far away from Earth. An example of one such location that is being considered is the Sun-Earth L2 point³.

OLFAR will be an interferometer consisting of approximately 50 satellites, spaced up to 100 km apart.

To keep both production and launch costs low, the satellites need to be small. Therefore, an OLFAR satellite will be based on the three-unit CubeSat platform⁴, which means the body is only 10×10×30 cm. This small format places constraints on the solar panel surface, and hence on the available power, but also on the size of all the sensors, actuators and internal parts of the satellite. This goes for the astronomic observation antennas as well. The current design of these antennas is a set of three deployable perpendicular dipoles^{5,6}.

As with any radio telescope, the OLFAR telescope will need to be calibrated, because the received signals will be corrupted by several factors. Examples are variations in the gain and phase of the receivers, the (imperfect) antenna patterns, the error in the attitude determination (position and orientation of the satellites) and receiver noise. The effect that all these factors have on the received signals needs to be estimated and compensated for to be able to obtain an accurate picture of the celestial sphere. That is the goal of calibration.

In this paper a calibration approach for the OLFAR radio telescope is proposed using an alternating least squares optimization (ALS) technique. The sky model is considered known and consisting of strong calibrators. Monte Carlo simulations are performed to provide proof of concept.

In the next section, the corrupting factors mentioned above and the challenges they pose specifically for OLFAR are looked into in more detail. In Section III, an approach to the calibration is proposed and studied in detail. The results of some preliminary simulations are presented in Section IV, and in Section V the conclusions will be presented.

II. OLFAR-SPECIFIC CHALLENGES

The two driving advantages of placing OLFAR in space, are the absence of the ionosphere and the distance from Earth-bound radio sources that cause radio frequency interference (RFI). Both these problems appear to be prohibitive for radio astronomy to be performed on Earth at frequencies below 30 MHz. By placing the radio telescope in space, the ionosphere is no longer a factor, and the RFI problem becomes much smaller², enabling observations at those low frequencies.

However, using a swarm of small satellites to implement a radio interferometer poses a host of new challenges for the calibration. The antennas are not fixed to the ground as in a traditional radio telescope, but they are floating in free space, where it cannot be assumed that the orientations of the satellites are identical. This means that the antenna gains towards one source are going to vary from satellite to satellite. There will be orientation sensors on the satellite, such as sun sensors or star trackers, but their accuracy might not be enough to support accurate imaging. This also poses a challenge for polarimetry, since the polarizations of the antennas on each satellite will be different.

The OLFAR satellites will fly in a swarm, meaning that the positions of the satellites are random in three dimensions. While an algorithm has been developed to estimate satellite positions and motions within the swarm using the inter-satellite communication system⁷, it might still be needed to improve the knowledge of the formation through the calibration algorithms.

The small size of the satellites also brings along a set of challenges. There is no room for large dishes, and during launch, the satellites need to fit within the ISIPOD deployer for the three-unit CubeSat⁴, so any antenna that is large enough to be sensitive to these low frequencies will need to be deployable so that it can be stored inside the ISIPOD deployer. The current design of the astronomical antennas is therefore a set of six 4.8 m long deployable wire antennas that extend from the satellite body, as is illustrated in Figure 1. Opposing pairs of these antennas are connected to the same receiver, forming three perpendicular dipoles. However, as can be seen from Figure 1, one set of monopoles is not perfectly aligned. This is because only one antenna can be deployed from each corner of the satellite body. This misalignment skews the antenna pattern^{5,6}. Besides

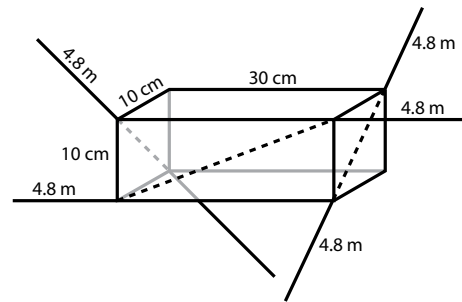


Fig. 1: Layout of the astronomical antennas on OLFAR. (Not to scale.)

the misalignment, this same monopole pair will be connected to separate receiver front-ends, and will be combined digitally, instead of being connected to a single receiver, as with the other two dipoles. The reason for this is that finding a route for a coaxial cable through the length of the satellite body is difficult, and it would be very easy for the electrical hardware in the satellite body to induce crosstalk into the cable. This means there will be two separate receiver gains, which if they do not match, might influence the performance and antenna pattern of this dipole as well.

OLFAR will have a view of the full celestial sphere at all times, and with the three dipoles, this means an omnidirectional field of view (FoV). With no means to focus the FoV, OLFAR will not be able to use a single calibrator source for calibration. OLFAR is not alone in this. For instance the Earth-based radio telescope LOFAR (Low-Frequency Array for Radio Astronomy) has the same property to a large extent, as it observes the half of the celestial sphere (a hemisphere) when performing snapshots with a single station⁸. However, calibrator sources are still useful in OLFAR, as they provide known parameters which can be used to fit the parameters to be calibrated to the observation.

The small satellite body, the difficulties in dissipating heat in vacuum, and the limited available power all mean that the computational capacity in an OLFAR satellite will be limited. High-end processors cannot be used, and what can be used and fits inside the body might have to run with a lower clock speed than it normally would on Earth. This means that the calibration should happen as much as possible on Earth, preferably using the measured data that OLFAR sends to Earth after observation and data reduction (correlation of the signals).

III. CALIBRATION APPROACH

In an interferometer such as OLFAR, all correlations between the signals from all antenna elements are

estimated using the formula

$$\hat{r}_{p_1 p_2} = \frac{1}{T} \int_0^T x_1(t) \overline{x_2(t)} dt \quad (1)$$

where T is the snapshot integration time, $x_1(t)$ and $x_2(t)$ the complex envelope of the received signals from receivers p_1 and p_2 , respectively, the over-bar denotes complex conjugation, and the circumflex denotes a measured quantity. The resulting data set is intuitively put into a P by P matrix $\hat{\mathbf{R}}$, (where P is the number of antennas), called the measured covariance matrix. This matrix contains all the correlation estimates between all antennas and is Hermitian.

This measured covariance matrix, together with orientation sensor readouts and satellite positions calculated from the ranging algorithms⁷, is the only information available on Earth. The received signals $x_p(t)$ are not available on earth, because this is a much larger data set than $\hat{\mathbf{R}}$, and the communication bandwidth to Earth is limited⁹. Furthermore, calibration can only be performed on earth because of the limited computational capacity in the satellites.

The goal is therefore to estimate how the measured covariance matrix $\hat{\mathbf{R}}$ was affected by the various factors and parameters which we need to calibrate, based on the available information on Earth. These parameters include

- complex amplitude gains of the receivers (which are direction independent) \mathbf{g} ;
- direction dependent antenna amplitude gains (due to the antenna patterns and satellite orientations) \mathbf{G}_0 ;
- satellite positions $\boldsymbol{\xi}$;
- satellite orientations $\boldsymbol{\xi}_L$;
- source powers $\boldsymbol{\sigma}_s$;
- source positions/direction of incidence \mathbf{e}_q ;
- receiver noise $\boldsymbol{\Sigma}_n$.

Fortunately this is possible since every element in $\hat{\mathbf{R}}$ is an observation of the sky as measured by a different pair of antennas. Comparing the elements of $\hat{\mathbf{R}}$ therefore holds information on the parameter values of those antennas and receivers. That is essentially what the calibration approach does.

In order to estimate these parameters from the measured data, a model is needed in the form of an equation that starts with the source parameters, incorporates all the parameters to be calibrated in the system, and has the covariance matrix as a result. This is called the measurement equation (ME)

$$\mathbf{R}(\boldsymbol{\theta}) = \text{ME}(\boldsymbol{\theta}) = \text{ME}(\mathbf{g}, \mathbf{G}_0, \boldsymbol{\xi}, \boldsymbol{\xi}_L, \boldsymbol{\sigma}_s, \mathbf{e}_q, \boldsymbol{\Sigma}_n)$$

where $\boldsymbol{\theta}$ represents the complete collection of parameters.

Then the goal of the calibration is to find the system parameters that let the output of the ME, \mathbf{R} , to as closely as possible resemble the measured covariance matrix, $\hat{\mathbf{R}}$. This can be done using a maximum likelihood (ML) formulation, an alternating least squares (ALS) approach or an extension thereof, weighted alternating least squares (WALS). These are presented in Section III.II.

In this paper it is assumed that the sky is dominated by several strong calibrator sources, the position and strength of which are known, i.e. a known sky model is assumed.

III.I Measurement Equation

To present the ME, we start with a simplified version, and then add each symbol that will appear in the final ME one by one, explaining them in turn so that the ME will become intuitively appealing.

The first symbol to be looked into represents the source powers. The sky model has Q sources, the powers of which are contained in the vector $\boldsymbol{\sigma}_s = [\sigma_1 \dots \sigma_q \dots \sigma_Q]$. Since the output of the ME is a covariance matrix, it is most convenient to represent the source signals in a covariance matrix as well. However we will assume that the source signals are all independent, resulting in a diagonal matrix $\boldsymbol{\Sigma}$ with the source powers on the main diagonal, i.e.

$$\boldsymbol{\Sigma}_s = \text{diag}(\boldsymbol{\sigma}_s). \quad (2)$$

A signal from a given source arrives at each satellite with a different delay because of the different satellite positions. This can be stored in the P by Q array response matrix \mathbf{A} . Note that this matrix consists of sets of three identical elements since every satellite has three co-located dipole antennas. The ME works with a complex representation and narrowband signals, so that a delay can be represented by a phase shift, i.e. by a multiplication by $\exp(j\phi)$, where ϕ is the phase. This means that each element of \mathbf{A} is given by

$$a_{pq} = \exp(j\phi_{pq}) = \exp(j 2\pi f_c c \boldsymbol{\xi}_p \cdot \mathbf{e}_q) \quad (3)$$

where c is the speed of light, f_c the observation frequency, $\boldsymbol{\xi}_p$ is the position of satellite p and \mathbf{e}_q a unit vector pointing towards source q , both in three-dimensional Cartesian coordinates. \mathbf{A} is combined with (2) to get the ME of an idealized interferometer with isotropic antennas,

$$\mathbf{R}' = \mathbf{A} \boldsymbol{\Sigma}_s \mathbf{A}^H$$

where \mathbf{R}' is a P by P covariance matrix, the prime denoting that the ME is not yet complete, and the superscript H denoting the Hermitian inverse. Each element of \mathbf{R}' is given by

$$r'_{p_1 p_2} = \sum_{q=1}^Q a_{p_1 q} \sigma_q \overline{a_{p_2 q}}.$$

In this equation the signals from each source are correlated separately before being summed. This is allowed since the signals from distinct sources are additive at the antennas, so the covariances resulting from different sources are additive as well. This means that for each source, one can simply take the autocorrelation (power) σ_q of a source and rotate it according to the delays $a_{p_1 q}$, and $\overline{a_{p_2 q}}$, where the latter needs to be conjugated as per the operation of correlation in described in (1).

Now we need to add the system parameters, starting with the direction dependent antenna amplitude gains. Due to the antenna patterns, every antenna has a different gain towards each source, so they are stored in the matrix \mathbf{G}_0 of size P by Q . This is the same size as \mathbf{A} , and implementation in the ME is therefore straightforward:

$$\mathbf{R}' = (\mathbf{G}_0 \odot \mathbf{A}) \boldsymbol{\Sigma}_s (\mathbf{G}_0 \odot \mathbf{A})^H$$

where \odot denotes element-wise multiplication.

Note that in OLFAR, the direction dependent gains are heavily dependent on the orientation of the satellites, $\boldsymbol{\xi}_z$. If the antenna patterns are known, this can be used together with $\boldsymbol{\xi}_z$ to calculate \mathbf{G}_0 . However, this can only be used as an initial guess during calibration, as component spread in the antennas or errors in the antenna pattern models will cause errors in the calculated \mathbf{G}_0 .

The next parameter to be implemented is the complex amplitude gains of the receivers \mathbf{g} , which is a vector of length P , with complex values, as the delay in the receiver chain is also a very important parameter in interferometry. The gains are put in a diagonal matrix, as $\mathbf{G} = \text{diag}(\mathbf{g})$, so we can add it to the ME. The off-diagonal entries of \mathbf{G} can be used to add mutual coupling (crosstalk) between signal paths, in which case \mathbf{G} is assumed to be Hermitian. In OLFAR, crosstalk is only expected between the receiver paths within one satellite. However calibrating for crosstalk is beyond the scope of this paper. Adding \mathbf{G} to the ME, we get

$$\mathbf{R} = \mathbf{G}(\mathbf{G}_0 \odot \mathbf{A}) \boldsymbol{\Sigma}_s (\mathbf{G}_0 \odot \mathbf{A})^H \mathbf{G}^H.$$

The last parameter to add is receiver noise. This is modelled as additive Gaussian noise and can be

represented by the P by P covariance matrix $\boldsymbol{\Sigma}_n$. If all the noise in all receivers is independent, $\boldsymbol{\Sigma}_n$ will be a diagonal matrix. However if there is a noise source that couples into more than one signal path (possibly within one satellite) then $\boldsymbol{\Sigma}_n$ will have off-diagonal non-zero values. In this paper however, we will assume that all receivers have equal and uncorrelated noise, so that $\boldsymbol{\Sigma}_n = \sigma_n \mathbf{I}_P$, where \mathbf{I}_P is the $P \times P$ identity matrix.

Since the receiver noise is additive, $\sigma_n \mathbf{I}_P$ becomes a separate term in the ME, giving the completed ME as

$$\mathbf{R} = \mathbf{G}(\mathbf{G}_0 \odot \mathbf{A}) \boldsymbol{\Sigma}_s (\mathbf{G}_0 \odot \mathbf{A})^H \mathbf{G}^H + \sigma_n \mathbf{I}_P \quad (4)$$

where the constituents of \mathbf{A} are given by (3).

Note that in the ME, \mathbf{G} and $(\mathbf{G}_0 \odot \mathbf{A})$ can exchange a common magnitude factor and a common phase without influencing \mathbf{R} . This becomes problematic when comparing parameters with the true values in simulations, or if multiple snapshot observations are combined to create a clear image of the sky. This means a constraint is needed on both the magnitude and phase to avoid these problems. The constraint chosen here for the magnitudes is that the average receiver gain magnitude is fixed, as it is known by its design. Another possibility would be to consider the maximum gain in the antenna patterns to be known and fixed, but the accuracy thereof would depend on the orientations of the satellites relative to the sources. The phase constraint is that the average receiver gain phase is 0 rad, which is possible when the phases do not vary too much from receiver to receiver. Simply defining the phase of one receiver to be 0 and using that as a reference as is commonly done^{8,10} is not practical here because the relative antenna locations are not fixed in OLFAR.

III.II Optimization techniques

There are several ways in which the model parameters can be estimated. An asymptotically efficient method is the maximum likelihood (ML) formulation. However, it appears that the ML formulation for this problem cannot be solved in closed form^{8,11}. A more tractable alternative is a least squares approach in which the total error squared is minimized, according to the cost function⁸

$$\kappa(\boldsymbol{\theta}) = \|\hat{\mathbf{R}} - \mathbf{R}(\boldsymbol{\theta})\|_F^2 \quad (5)$$

where $\boldsymbol{\theta}$ represents the complete set of parameters to be estimated, $\|(\cdot)\|_F$ denotes the Frobenius norm and $\mathbf{R}(\boldsymbol{\theta})$ is given by (4). Because $\boldsymbol{\theta}$ consists of many different kinds of parameters, such as the different kinds of gains and phases, the cost function is minimized only for subsets of the parameters at a time, alternating between all subsets. This approach is known as the alternating least squares (ALS) method which will be studied in

detail in the next subsection. An extension of ALS is weighted ALS (WALS). In WALS, weights are given to each data point (i.e. each element of \mathbf{R}) that determines its influence on the parameter estimation, which can improve the estimation accuracy. However, the implementation of WALS for the calibration problem at hand is beyond the scope of this paper.

Alternating Least Squares (ALS) Optimization

An ALS approach has been developed for the calibration of OLFAR, based on (4). The complete set of parameters θ is divided in five subsets:

- the elements of the array response matrix $a_{pq} = \exp(j\phi_{pq})$;
- the phases of the receiver gains $\arg(g_p)$;
- the magnitudes of the receiver gains $|g_p|$;
- the direction dependent gains $g_{0,pq}$;
- the receiver noise powers σ_n .

Least squares solutions are found for each set of parameters in turn, while the rest of the parameters are fixed to their current estimate or initial guess. ALS alternates between these sets, iterating towards a global least-squares solution for all parameters, until a stopping criterion is reached.

The parameters listed above can be divided in two categories: phases ($\arg(g_p)$ and ϕ_{pq}) and magnitudes ($|g_p|$, $g_{0,pq}$ and σ_n). For the magnitudes it can be observed that the ME in (4) is approximately linear. This is illustrated below by looking at the receiver gains \mathbf{G} in the ME, but for all other magnitude parameters a similar argument can be made. If we ignore receiver noise for the moment, for a single entry in \mathbf{R} we have

$$r_{p_1,p_2} = g_{p_1}g_{p_2} \sum_{q=1}^Q g_{0,p_1q} a_{p_1q} \sigma_q g_{0,p_2q} \overline{a_{p_2q}}. \quad (6)$$

This equation is linear in g_{p_1} as long as $p_1 \neq p_2$, a condition that holds everywhere in the ME, except on the diagonal. If the diagonal is ignored, finding a least squares solution for the magnitude parameters is a standard linear least squares problem, with a single minimum in the cost function.

Since the diagonal is only a small part of \mathbf{R} , when it is included in the minimization the nonlinearity is small enough so that it does not create local minima. The minimum can then be found within a few iterations of a linear least squares algorithm. However, the receiver noise is much stronger than the celestial sources. This makes the diagonal a very unreliable source of information for the estimation of any gain, because the noise term is dominant on the diagonal. Ignoring the diagonal could therefore improve the estimation of the

direction independent gains as a result of this, which has been confirmed in simulation (see the next section). Ignoring the diagonal in this way could be seen as a primitive form of WALS, where the diagonal entries are given weight 0, and all other elements are given weight 1.

By similar arguments as for $|g_p|$, it can be shown that (4) is mostly linear in a_{pq} as well. However, in the case of the array response matrix we are interested in their phases ϕ_{pq} , for which the ME is harmonic rather than linear. This means that (6) can be rewritten as a function of ϕ_{pq} as

$$r_{p_1,p_2}(\phi_{p_1q_1}) = A + B \exp(j\phi_{p_1q_1})$$

where A and B are constants which are given by

$$A = \begin{cases} g_{p_1}g_{p_2} \sum_{\substack{q=1 \\ q \neq q_1}}^Q g_{0,p_1q} a_{p_1q} \sigma_q g_{0,p_2q} \overline{a_{p_2q}} & \text{for } p_1 \neq p_2 \\ g_{p_1}g_{p_2} \sum_{q=1}^Q g_{0,p_1q} a_{p_1q} \sigma_q g_{0,p_2q} \overline{a_{p_2q}} & \text{for } p_1 = p_2 \end{cases}$$

and

$$B = \begin{cases} g_{p_1}g_{p_2}g_{0,p_1q_1}\sigma_{q_1}g_{0,p_2q_1}\overline{a_{p_2q_1}} & \text{for } p_1 \neq p_2 \\ 0 & \text{for } p_1 = p_2 \end{cases}.$$

Note that when $p_1 = p_2$ and $q = q_1$, we get a term that is independent of $\phi_{p_1q_1}$ since $a_{p_1q_1}\overline{a_{p_1q_1}} = 1$, and hence it becomes part of the constant A for $p_1 = p_2$. This means the function will only have a single minimum within the interval $0 < \phi_{pq} < 2\pi$. When inserted into (5), the single minimum will remain at the same value for ϕ_{pq} as long as $\kappa(\theta) > 0$ for all ϕ_{pq} , which in all practical scenarios will be true because of model inaccuracies and the finite integration time. It is then possible to locate that minimum very quickly. Take four samples of $\kappa(\theta)$ at ϕ_{pq} equals 0, 0.5π , π and 1.5π , take the fast-Fourier transform (FFT) of the resulting sequence and look at the phase of the second frequency sample, the one representing the ground harmonic.

By similar arguments, this technique can be applied to the phases of the receiver gains as well.

IV. SIMULATIONS

To verify the proposed calibration technique, Monte Carlo (MC) simulations have been performed. For each MC run a new satellite swarm with a new sky model has been generated. With each iteration the number of

Swarm	
Number of satellites	50
Number of antennas/receivers per satellite	3
Total number of antennas/receivers, P	150
Swarm distribution	Gaussian
Swarm diameter (95% inside)	0.3 km
Satellite orientations	Random
Receiver gain (magnitude - mean)	1
Receiver gain (magnitude - variance)	0.03
Receiver gain (phase - variance)	0.03 rad ²
Receiver noise power (only different for each MC run)	equal in all receivers
Average receiver noise power	See: Table 2
Variance of receiver noise power	5
Integration time	See: Table 2
Bandwidth of correlated signal	1 kHz
Sky Model	
Number of point sources, Q	3
Source directions	Random
Source powers (received power)	uniform within (0.5 ; 1)

Table 1: Parameters and assumptions for the Monte Carlo simulations.

satellites has been the same, as well as the number of point sources in the sky model. All other parameters are randomly generated according to the assumptions and parameter values listed in Table 1. Since in the MC simulation we are interested in the accuracy of the calibration, the absolute value of the source powers are not relevant. However the ratio between the received source powers and the noise powers in the receiver is important, as this does influence the accuracy. For this reason the powers are expressed as unitless quantities in Table 1 and in the remainder of the paper.

Because of the way the satellite positions and sky models are randomized in the simulations, there is no statistical difference between the accuracy of the calibration routine between parameters of different antennas or satellites. Therefore, when estimating the accuracy of for instance the receiver gains, all the errors can be averaged for all the gains to get an estimate for the accuracy within one MC run. Because of this, convergence in the MC simulations is a lot faster, except for the receiver noise σ_n , since it is only one parameter for each MC run. In this light, the outcome of

Simulation conditions				Unit
Receiver noise power	10 ³	10 ⁴	10 ⁴	relative
Integration time	1	1	4	seconds
Error variance of parameters				Unit
Receiver gains (magnitude)	1.8·10 ⁻³	85·10 ⁻³	15·10 ⁻³	relative
Receiver gains (phase)	11·10 ⁻³	19·10 ⁻³	13·10 ⁻³	radian ²
Antenna gains	2.5·10 ⁻³	0.13	14·10 ⁻³	relative
Array response matrix	12·10 ⁻³	22·10 ⁻³	14·10 ⁻³	radian ²
Receiver noise	1.6·10 ⁻³	1.5·10 ⁻³	1.7·10 ⁻³	relative

Table 2: Results of the Monte Carlo simulations.

the MC simulation is only five error variance values, one for each subset of parameters listed in Section III.II.

IV.I Simulation results

The results of three MC simulations are summarized in Table 2. In the final result, some MC runs have been removed from the data set. This seemed to be necessary as in those cases the runs in question produced error variance outliers of one to four orders of magnitude above the rest. These outliers are believed to be caused by the numerical approximations involved in the linear least squares solver, causing the optimization routine to become numerically unstable and diverge. The signal-to-noise ratio (SNR) in the measured covariance matrix $\hat{\mathbf{R}}$ also seems to have an influence on this. In the simulation where the noise power was 10⁴, with 1 second integration time, about 3% of the MC runs were discarded. With the integration time increased to 4 seconds, the amount of runs discarded was 1.5%, while when the noise power was 10³, none of the MC runs were discarded.

As mentioned in Section III.II, the diagonal entries were ignored for the gains, as this appears to give an improvement of up to 20% of the estimation error variance, as well as fewer problems with numerical instability.

When looking at Table 2, it can be seen that the parameters are estimated with decent accuracy as long as the SNR is not too low. It shows that a large receiver noise power has a negative influence on the accuracy of the calibration, while choosing a longer integration time improves the situation. This is an intuitively appealing result, as both factors affect the SNR on the measured covariance matrix.

V. CONCLUSIONS

A calibration routine was developed for the OLFAR radio telescope that estimates the complex receiver

gains, the array response matrix and the direction dependent antenna gains towards the calibrator sources, based on a sky model consisting of known strong calibrator sources. The calibration routine is based on alternating least squares (ALS) optimization, and was verified using Monte Carlo (MC) simulations. While some MC runs had to be discarded due to occasional numerical instability of the calibration routines, the routines do successfully show that calibration of a radio telescope consisting of a swarm of small satellites is possible with a least-squares approach. In future work,

the problems with numerical instability do need to be solved or at least better understood, and the calibration should be refined and extended in the future to become more general.

Acknowledgements

This work is part of the DCIS (Data Collecting Colonies in Space) project, which is supported by NanoNextNL, a micro and nanotechnology consortium of the Government of the Netherlands and 130 partners.

-
- ¹ M. J. Bentum, C. J. M. Verhoeven, and A. J. Boonstra, "OLFAR - orbiting low frequency antennas for radio astronomy," in *20th Annual Workshop on Circuits, Systems and Signal Processing, ProRISC 2009, Veldhoven*, pp. 1–6, Technology Foundation STW, November 2009.
 - ² S. Jester and H. Falcke, "Science with a lunar low-frequency array: From the Dark Ages of the universe to nearby exoplanets," *New Astronomy Reviews*, vol. 53, no. 12, pp. 1 – 26, 2009.
 - ³ R. Rajan, S. Engelen, M. Bentum, and C. Verhoeven, "Orbiting low frequency array for radio astronomy," in *Aerospace Conference, 2011 IEEE*, pp. 1 – 11, March 2011.
 - ⁴ California Polytechnic Institute, "CubeSat Design Specification," Revision 12, August 2009.
 - ⁵ K. Quillien, S. Engelen, D. Smith, M. Arts, and A.-J. Boonstra, "Astronomical antenna for a space-based low frequency radio telescope," *27th Annual AIAA/USU Conference on Small Satellites*, 2013.
 - ⁶ D. Smith, M. Arts, A.-J. Boonstra, and S. Wijnholds, "Characterisation of astronomical antenna for space based low frequency radio telescope," in *2013 IEEE Aerospace Conference*, pp. 1 – 9, March 2013.
 - ⁷ R. Rajan and A.-J. van der Veen, "Joint motion estimation and clock synchronization for a wireless network of mobile nodes," in *2012 IEEE International Conference on Acoustics, Speech and Signal Processing (ICASSP)*, pp. 2845–2848, March 2012.
 - ⁸ S. Wijnholds, *Fish-eye observing with Phased Array Radio Telescopes*, PhD thesis, TU Delft, Dept. EEMCS, March 2010. ISBN 978-90-9025180-6.
 - ⁹ A. Budianu, A. Meijerink, and M. J. Bentum, "Swarm to earth communication in OLFAR," in *Proceeding of the 64th IAC International Astronautical Congress, Beijing, China*, (Beijing, China), pp. 1–6, International Astronautical Federation (IAF), September 2013.
 - ¹⁰ R. A. Thompson and Et, *Interferometry and synthesis in radio astronomy*. Wiley-Interscience, 1998. ISBN 1-57524-087-4.
 - ¹¹ B. Ottersten, P. Stoica and R. Roy. "Covariance Matching Estimation Techniques for Array Signal Processing Applications," *Digital Signal Processing, A Review Journal*, 8:185–210, July 1998.